



HIGH TEMPERATURE PROCESSING OF COMPLEX ORES

From Ore Body to High Temperature Processing of Complex Ores: Manganese—A South African Perspective

JOALET DALENE STEENKAMP ^{1,2,3} DESHENTHREE CHETTY,¹
ASHMA SINGH,¹ SUSANNA ALETTA CAROLINA HOCKADAY,¹
and GLEN MICHAEL DENTON¹

1.—MINTEK, Johannesburg 2125, South Africa. 2.—University of the Witwatersrand, Johannesburg 2001, South Africa. 3.—e-mail: joalets@mintek.co.za

Manganese is considered a relatively rare metal as concentrations of it in ore of commercial importance are geographically limited. In nature, manganese is found in the form of oxides, carbonates, and silicates. Manganese ores are complex in the sense that they not only consist of a complex oxide mineral assemblage but these minerals are also very finely inter-grown. South Africa accounts for 74% of the world's identified manganese resources and 32% of the world's reserves. The paper presented here describes in more detail the resource and the complex mineralogy of the ore body, as well as the existing and potentially new processing technologies available from minerals processing and pyrometallurgical perspectives.

INTRODUCTION

Manganese is the 12th most abundant element in the Earth's crust, with an average concentration of 0.1%.¹ It was recognized and isolated as a separate chemical element in 1774 by Carl Wilhelm Scheele and Johan Gottlieb Gahn.² Relatively rare metals are defined as: 'geochemically relatively scarce, having an upper crustal abundance < ~ 0.025 mass%' or 'subject to national stockpiling to prevent shortages in alloy production'.³ Concentrations of manganese in ore of commercial importance are geographically limited, and countries, including the USA,⁴ manage national stockpiles of ore and alloys. Therefore, manganese is considered a relatively rare metal.

In nature, manganese is found in the form of oxides, carbonates, and silicates both on land and in sea nodules.^{1,2,5,6} Manganese ores are complex in the sense that they not only consist of a complex oxide mineral assemblage but these minerals are also very finely inter-grown. As South Africa accounts for 74% of the world's identified manganese resources and 32% of the world's reserves,⁴ the paper presented here describes in more detail

the resource and the complex mineralogy of the ore body, and the existing and potentially new processing technologies available, both from minerals processing and pyrometallurgical perspectives.

MANGANESE AS COMMODITY

Historic Applications

Manganese was utilized by the Spartans, in ancient Greece, in their steel weapons to give superior strength. The Romans and Egyptians utilized manganese compounds to remove or add color to their glass during glassmaking,¹ as is still done today.⁵ In ancient China, manganese was utilized in glazes to give pottery an eggplant color.⁷ The first commercial use of manganese during the industrial revolution was as the laboratory reagent, KMnO_4 , which was produced for the first time by Johann Glauber in 1659.¹ MnO_2 was utilized in the manufacture of chlorine in the mid-18th century.²

As a commodity, large-scale consumption of manganese started when Sir Henry Bessemer introduced manganese as a deoxidizing agent in the eponymous steelmaking process for which he was awarded an English patent on October 17th, 1855.⁸ He initially added, after the oxygen blow, *spiegeleisen* (8% Mn, 4% C, and 86% Fe) and, from 1862 onwards, what he called ferromanganese (20–25% Mn), to remove oxygen from the steel and to add

manganese and carbon. He claimed to have based the application on expired patents obtained by William Reynolds in 1799⁹ and Josiah Marshall Heath in 1839¹⁰ and not on patents applied for by Robert Mushet on September 16th and 22nd, 1856.⁸ This paved the way not only for modern steelmaking, but also for the modern production of manganese ferroalloys.¹

Manganese Ferroalloys

Manganese ferroalloys produced commercially can be divided into the following three categories,¹ which are listed, together with their typical chemical compositions, in Table I: high carbon ferromanganese (HCFeMn), refined ferromanganese or medium carbon ferromanganese (MCFeMn), and silicomanganese (SiMn).

Of the manganese ferroalloys produced, 90% is utilized in steelmaking¹ where manganese is added to steel in order to:

- Deoxidize the steel, i.e., remove oxygen from the steel as MnO, although silicon and aluminum are stronger deoxidizers. Silicon deoxidizes steel and manganese enhances the effect of silicon deoxidation by forming stable manganese silicates and aluminates.¹
- React with sulfur to form MnS instead of FeS. At hot rolling temperatures of 900–1100°C steel becomes brittle due to the formation of liquid FeS on grain boundaries. The phenomenon is referred to as *cassant à chaud* (hot shortness) or *red-shortness*.⁸ MnS remains solid at hot rolling temperatures.¹¹
- Influence the strength, toughness and hardness of the steel.¹

Other Applications

Other applications of manganese include electrolytic manganese metal utilized primarily in alloys of aluminum and copper where it improves the corrosion resistance of aluminum.¹ Potassium permanganate (KMnO₄) is utilized as a disinfectant, deodorant, and as a bleaching and analytical reagent.² Manganese sulfate (MnSO₄) is utilized as a fertilizer, especially in citrus production, and as a reducing agent in the manufacture of paint and varnish driers.² Manganosite (MnO) is utilized as a

raw material in the production of manganous salts, an additive in fertilizers, and a reagent in textile printing.² Manganese (II) chloride (MnCl₂) is utilized as a catalyst in the chlorination of organic compounds and as an additive to animal feed.² Manganese dioxide (MnO₂) is utilized in dry cell batteries, as a chemical oxidant in organic synthesis, and as a raw material in the production of chemical grade manganous oxide.²

KALAHARI MANGANESE FIELD

In South Africa, manganese was first discovered at Hout Bay near Cape Town in 1873 from where small quantities were mined and exported in 1917.¹² The Northern Cape Province of South Africa hosts manganese in the Kalahari Manganese Field (KMF), discovered at Black Rock in 1907, and in the Postmasburg Manganese Field. Mining in the Postmasburg area started in 1922 and in the KMF in 1954.¹³ As the KMF is the major resource from which Mn is derived in South Africa, this section describes this orebody specifically.

Geology

The KMF is the world's largest land-based repository of manganese, located ~ 60 km north-northwest of the town of Kuruman in the Northern Cape Province of South Africa. The deposit consists of five erosional relics of the Hotazel Formation (Fig. 1): the Kalahari Manganese Deposit (KMD), the Avontuur and Leinster basins to the north thereof, and the mined out Hotazel and Langdon-Devon deposits hosted in grabens to the east of the KMD. Of these, the KMD is by far the largest, covering an area of maximum dimensions 41 × 20 km (~ 320 km² underlain). The Hotazel Formation consists of intercalations of banded iron formation (BIF) and hematite lutites with a series of three manganese ore layers: the lower, middle, and upper layers. The lower layer has traditionally been the focus of mining, given its well-developed nature throughout the deposit, reaching a maximum thickness of 45 m in the Mamatwan Mine to the southeast. The uppermost layer is typically lower in grade, and poorly developed, at around 2 m in thickness, and commonly absent owing to erosional effects from other geological formations over time. Where the grade is good, this layer has received some attention previously. The middle layer is uneconomic and

Table I. Categories of manganese ferroalloys produced internationally and their typical chemical composition in mass% (balance Fe) as defined in ASTM-A99: Standard Specification for Ferromanganese and ASTM-A483: Standard Specification for Silicomanganese

Product	Mn	C	Si	Fe	P	S	Mn/Fe
HCFeMn	74–82	7.5	1.2	9.3–17.3	0.35	0.050	4.3–8.8
MCFeMn	80–85	1.5	0.35–1.5	12.0–18.2	0.30	0.020	4.4–7.1
SiMn	65–68	1.5–3.0	12.5–21.0	8.0–21.0	0.20	0.04	3.1–8.5

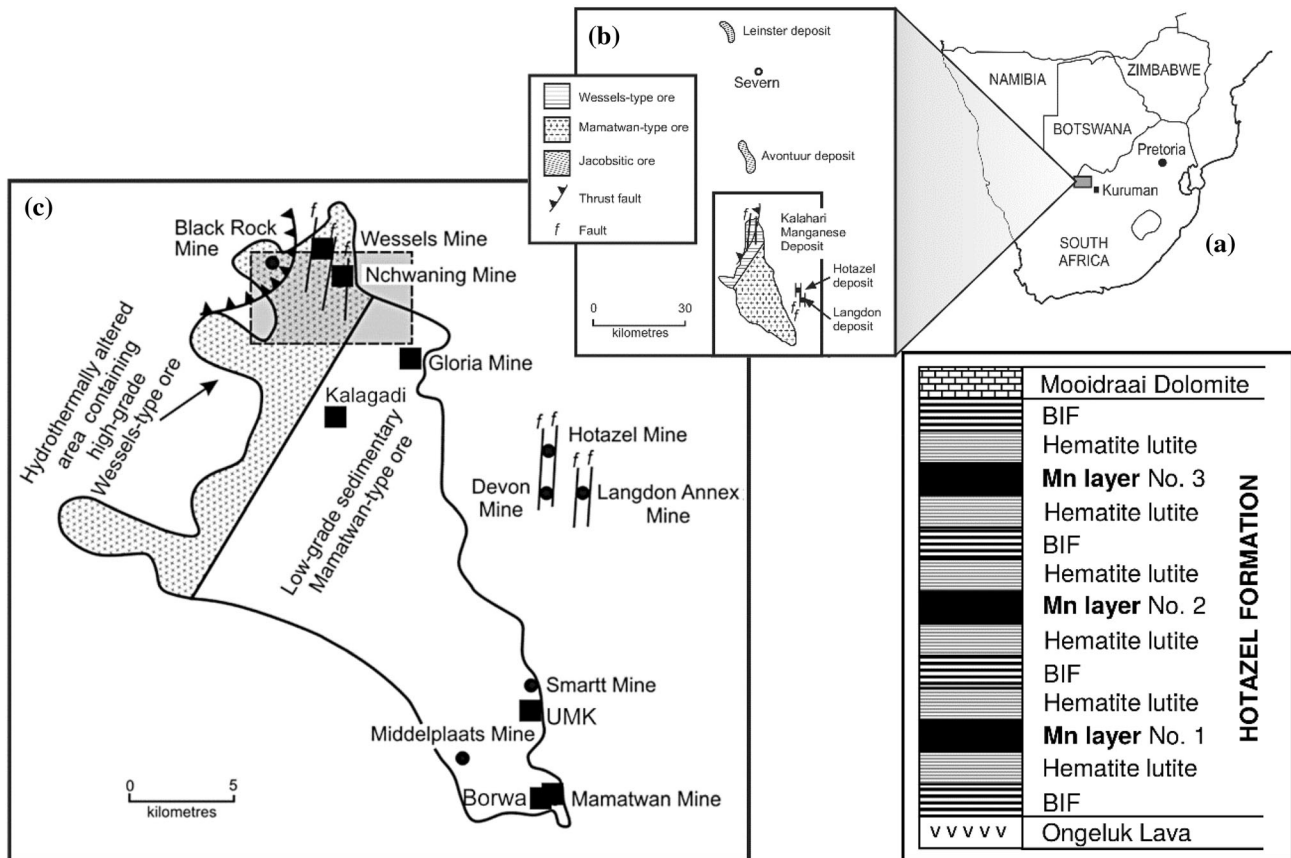


Fig. 1. (a) Locality of the KMF in South Africa; (b) map of the KMF, showing the five erosional relics of the Mn-bearing Hotazel Formation; (c) map of the KMD, showing current mining operations (squares) and historic operations (dots), with high-grade mining areas shown by the shaded rectangle in the north. A simplified stratigraphic column of the Hotazel Formation showing the three Mn layers is also shown on the right. Layer No. 1 is the lower layer and main orebody exploited. (Reprinted from Ref. 15)

< 1 m in thickness. Some exploration work has also been undertaken in the Leinster and Avontuur basins previously, although no production is taking place presently. The KMF ores are largely unexposed at surface level, with the Black Rock outcrop the only evidence of the ore exposed at surface.

Structurally, the Hotazel Formation, including the Mn ore layers, dips $\sim 8^\circ$ to the west,¹⁴ which has resulted in different mining approaches in different parts of the sub-outcrop area. The Mamatwan, United Manganese of Kalahari (UMK), and Tshipi Borwa operations, in the southern part of the KMD, are open-cast, owing to the near-surface occurrence of the ore, specifically the lowermost Mn ore layer. The middle and upper layers have been eroded away in this part of the deposit, and a geological unconformity exists between the lower Mn ore layer and younger sedimentary rocks of the Kalahari Formation, which are stripped as overburden in open-cast operations. Further north-west, however, the Kalagadi, Gloria, Nchwaning (I, II, II), and Wessels operations are underground mines, as the dipping ore layers are situated deeper underground in those parts of the deposit. Moving westwards, the uppermost layer is better preserved in the northern part of the KMD, with the lower layer

remaining the primary focus of mining underground.

In addition to the dip of the ore layers, the northern part of the KMD is beset by a series of north-south striking faults that have displaced the ores, causing alteration of the ore to form different mineral assemblages. A thrust fault in the western portion of the northern KMD caused the ore to protrude at the surface as the Black Rock outcrop. In the southern part of the KMD, faulting is minor; instead, the unconformity overlying the lower Mn ore layer has resulted in variable alteration to the ore, caused by meteoric fluids.^{16,17}

Ores

The principal types of ores that occur in the main KMF deposit are the low-grade, Mamatwan-type ore, and the high-grade, Wessels-type ore.¹⁸ Smaller concentrations of a supergene ore type occur in the southern margins of the KMD. The Mamatwan-type ore occurs throughout the KMD, but dominates the southern two-thirds of the deposit, whereas the Wessels-type ore is restricted to the northern portion of the deposit, particularly where the north-south striking faults occur.^{14-16,19} The supergene

altered ores occur in the southern portion of the KMD, where affected by the unconformity.¹⁷ In the northern KMD, some supergene alteration may occur in the uppermost ore layer.²⁰ A comparison of the three ore types is summarized in Table II.

The Mamatwan-type ore represents the protolith ore, known as manganese lutite, a carbonate-rich chemical sedimentary deposit that formed more than 2 billion years ago. The three layers were precipitated out in a marine environment as part of cyclic environmental patterns that precipitated BIF, hematite lutite, and Mn lutite, which, together, constitute the Hotazel Formation.²¹ At the Mamatwan mine, the lower layer is ~ 45 m in thickness.²² This ore is characterized by major amounts of dolomite-group carbonate, in the form of, predominantly, kutnahorite [Ca(Mg, Mn)(CO₃)₂] and braunite (Mn²⁺Mn³⁺SiO₁₂), the chief Mn-bearing oxide. Note that, although Si is part of the formula, this mineral is not a silicate, as silica comprises, at most, only 10% of the mineral.¹⁸

The Wessels type of ore formed as a result of hydrothermal alteration of the Mamatwan-type ore, an event that occurred around 1 billion years ago when fluids infiltrated through the normal faults in the northern KMD.^{14,23} These fluids dissolved away the carbonates, thus naturally upgrading the Mn oxides, leading to the high-grade ore typical of the Wessels type. The lower layer also decreases in thickness to around 4–8 m,¹⁴ an approximate ten-fold decrease compared with the protolith ore at Mamatwan. A much wider variety of minerals is encountered in this ore type, with Mn chiefly hosted by hausmannite, braunite II, and bixbyite.^{16,23}

The supergene ores represent a very small portion of the deposit, and contain Mn minerals with higher oxidation states of Mn compared with the other two types.¹⁷

Texturally, the Mamatwan-type ore is very fine-grained (typically < 5–20 μm), composed of mm-scale carbonate-rich laminae and ovoid features in a fine-grained matrix rich in braunite, along with hematite and hausmannite in subordinate quantities (Fig. 2a). The Wessels-type ore, on the other hand, can vary from fine grained [micron-scale grains (Fig. 2b and c)] to extremely coarse grained (mm-scale grains) assemblages. Supergene ores can likewise show variable grain size of the minerals in the assemblage, with cross-cutting veins of alteration minerals evident. The textural attributes of low-grade ores are particularly important in that some physical separation methods may be applicable for upgrading these ores through reduction of carbonate content. Furthermore, the upgrading of fines generated during crushing relies on textural attributes in determining whether sufficient Mn ore mineral liberation may be achieved to upgrade into saleable material.

Quantitative Mineral Abundance

From the high-temperature processing point of view, the mineralogical make-up of the ores is important to understand. Reactions in the pre-reduction zone of the furnace are likely to be different for different ore mineralogical compositions, as mineral reactions will have different energy requirements,²⁴ as well as different kinetics.²⁵ In Mn smelting operations in South Africa,

Table II. Grade, geographical distribution, resource %, and key minerals of ore types in the Kalahari Manganese Deposit^{16–19,23}

Mamatwan type	Wessels type	Supergene type
Low grade, 38% Mn	High grade, > 45% Mn	Intermediate grade, 38–45% Mn
Found throughout the KMD, dominates in the southern KMD	Restricted to the northern KMD	Found at unconformities where ores were exposed to meteoric fluids, e.g., south-eastern edge of the KMD, northern KMD
Makes up ~ 97% of the resource	Makes up ~ 3% of the resource	Makes up < 1% of the resource
Braunite, Mn ²⁺ Mn ³⁺ SiO ₁₂	Hausmannite, Mn ²⁺ Mn ³⁺ O ₄	Braunite, Mn ²⁺ Mn ³⁺ SiO ₁₂
Kutnahorite, Ca(Mn,Mg)(CO ₃) ₂	Bixbyite, (Mn,Fe) ₂ O ₃	Hausmannite, Mn ²⁺ (Mn ³⁺ ,Fe ³⁺) ₂ O ₄
Hausmannite, Mn ²⁺ (Mn ³⁺ ,Fe ³⁺) ₂ O ₄	Braunite II, Ca(Mn ³⁺ Fe ³⁺) ₁₄ SiO ₂₄	Manganomelane ^a , KMn ⁴⁺ Mn ³⁺ O ₁₆
Mn-calcite, (Ca,Mn)CO ₃	Hematite, Fe ₂ O ₃	Manganite, MnO(OH)
Hematite, Fe ₂ O ₃	Andradite, Ca ₃ Fe ³⁺ (SiO ₄) ₃	Pyrolusite, MnO ₂
	> 135 minerals, mostly trace in abundance	Todorokite, (Na,Ca,K) ₂ (Mn ⁴⁺ ,Mn ³⁺) ₆ O ₁₂ ·3–4.5(H ₂ O) calcite, CaCO ₃ dolomite, CaMg(CO ₃) ₂ quartz, SiO ₂

^aA group of supergene Mn minerals, for which the cryptomelane formula is presented

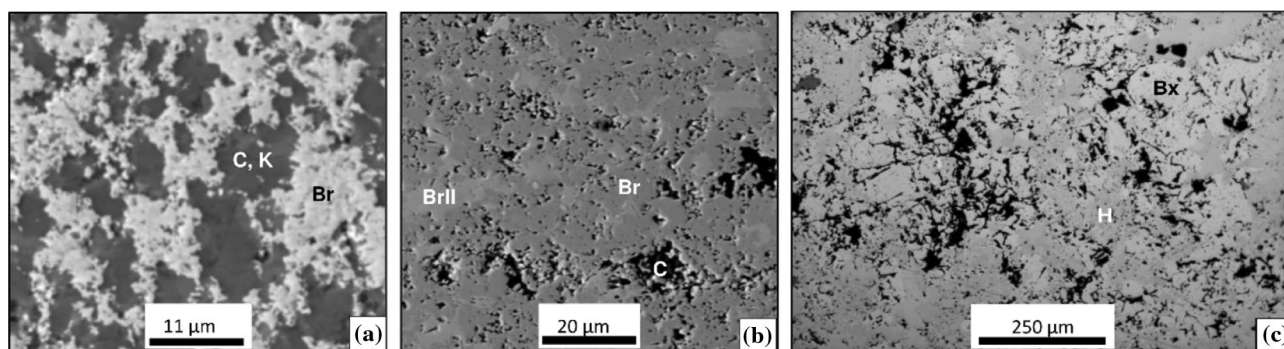


Fig. 2. Textures in low-grade and high-grade ores. (a) Back-scattered electron (BSE) image showing fine grained braunite (Br) inter-growths with carbonate (C = calcite, K = kutnahorite), Mamatwan-type ore; (b) BSE image showing braunite (Br) and braunite II (BrII) inter-growth with interstitial calcite (C), Nchwaning II; (c) plane polarized optical image showing hausmannite (H) replacing fractured bixbyite (B) grains, Nchwaning II (Reprinted from Ref. 23)

bulk chemical assays are typically relied on to adhere to specifications of the furnace charge. What is not known is how the Mn is distributed in different minerals. Chetty²³ and Chetty and Gutzmer¹⁹ cited a series of reactions to show the reduction path of Mn ore from MnO_2 to Mn in metallic form, in the presence of CO or C. The reduction of Mn^{4+} and Mn^{3+} occur with CO to form CO_2 and of Mn^{2+} only with C to form CO. The higher the oxidation state of the Mn, the more exothermic the reaction. The reduction of Mn^{2+} as well as the Boudouard reaction, where CO_2 reacts with C to produce CO, are both strongly endothermic reactions. The overall endothermic extent of the reduction process is therefore dependent on the extent of pre-reduction of Mn_3O_4 before the Boudouard reaction starts to take place at temperatures above $800^\circ C$. To this end, a method was developed to determine the bulk Mn oxidation state of KMD ores using quantitative mineralogy.^{15,19,23,26} Pulverized ores of the different types found in the KMD were subjected to x-ray diffraction analysis, with subsequent Rietveld refinement of the diffractogram outputs to quantify identified minerals. An extensive dataset of mineral chemical data has been established through electron probe microanalysis (EPMA) of various Mn containing minerals.^{15,23} Using the EPMA-derived Mn concentrations, as well as the mineral chemical formula, the Mn is partitioned at mineral chemical level into respective Mn valence states for each mineral. In much the same manner that a standard element deportment amongst minerals is determined, a valence deportment is carried out for Mn, to arrive at bulk Mn^{2+} , Mn^{3+} , and Mn^{4+} concentrations for samples of each ore type. The bulk valence state may be expressed as ratios of $Mn^{3+}:Mn^{2+}$ for Mamatwan- and Wessels-type ores. For supergene ores, this ratio may be $Mn^{4+}:Mn^{2+}$. In both cases, Mn^{2+} is expressed as unity. Figure 3 shows a plot of Mn valence states versus Mn ore grade.¹⁵

It is clear from the plots that a given Mn grade can return different bulk Mn oxidation states, based

on the proportion of minerals hosting higher valence Mn to those with lower valence Mn. In high-grade ores, the bulk Mn valence is determined by the proportion of the higher oxide, braunite group of minerals (braunite/brauniteII/bixbyite) relative to the lower oxide hausmannite content. Thus, such ores, whilst of similar Mn grade, will have different energy requirements.

Where ores display different grades, similar $Mn^{3+}:Mn^{2+}$ ratios may be observed. This is derived from different mineral assemblages (e.g., lower oxide kutnahorite-rich low-grade ores versus lower oxide hausmannite-rich high-grade ores) returning the same bulk Mn oxidation state. The similarity in the bulk Mn valence for very different mineralogy results from physicochemical conditions of alteration during the genesis of the deposit.²³

Supergene-altered ores also show different grades and bulk Mn oxidation states (Fig. 3). The ratios are dependent on the abundance of supergene oxides such as todorokite and manganomelane. Supergene alteration was found to be highly variable in the south-eastern margin of the KMD.¹⁷ Variation in mineralogy, associated bulk Mn oxidation state, and therefore energy needs, is thus also expected.

Quantitative mineralogy and the associated calculation of a bulk Mn oxidation state for ores may be applied as a routine analysis on assay pulps in understanding the effect of mineralogical variability on energy requirements in the furnace. This is particularly important in the hydrothermally altered, complex ores of the northern part of the KMD. The method is equally applicable for use on other Mn ores worldwide.

MINERALS PROCESSING

State of the Art

The steady rise in mining costs and escalating electricity prices²⁷ have necessitated South Africa to explore innovative ways of mining and downstream beneficiation to resolve the aforementioned challenges with the objective of growing and sustaining

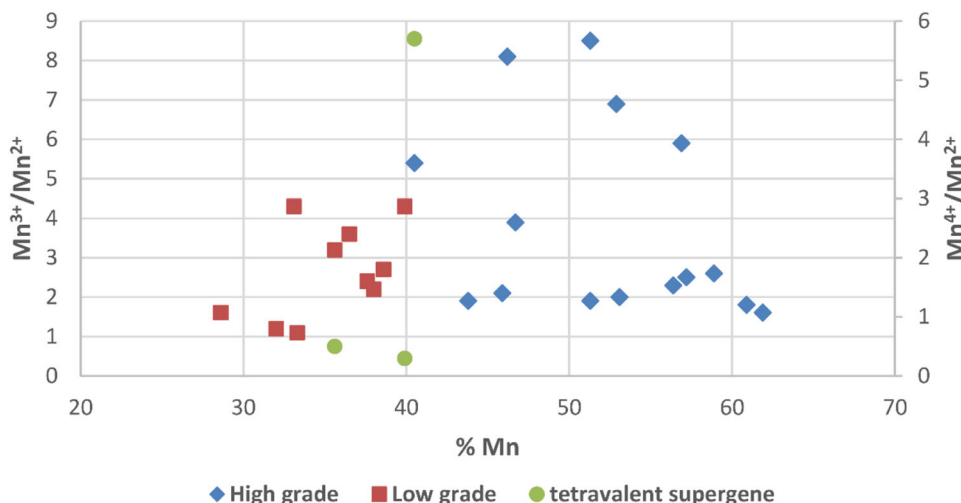


Fig. 3. Bulk Mn valence states plotted for various grades of Mn ores found in the KMD (Reprinted from Ref. 15)

the manganese mineral reserves. This section focuses primarily on the minerals processing initiatives (comminution and physical separation) aimed at reduced operational and capital costs, improved energy efficiency, and utilization of unexploited reserves. To accomplish the above-mentioned objectives, the current beneficiation technologies and future development trends within the manganese sector are reviewed.

Historic Processing

Historically and at present, mines within the KMD have been treating ores with Mn content > 38%. The volume output has thus been limited to available material. There exist opportunities to exploit unutilized, sterile resources about which mineralogical composition and information regarding liberation and gangue association is somewhat known. This would then enable ‘unlocking’ of a significant quantity of viable feed material for downstream applications.

The low-grade, Mamatwan-type ore containing carbonate or silicate gangue material, has traditionally undergone upfront waste rejection via dense media separation (DMS) or jigging. DMS or jigging methods are typically used for lumpy (9–75 mm²⁸) ores containing distinct coarse, liberated waste material displaying a density differential compared with the valuable manganese mineral.

The pre-concentrated product then further undergoes crushing and/or milling followed by a fines processing route entailing spiral, up-current classifiers and, where applicable, magnetic separation test work to increase the Mn/Fe ratio, thereby reducing the input material and slag produced during smelting.²⁹

To minimize waste dilution across extended mine operations and taking into account the complex nature of future ore bodies, selective mining has been employed. Therefore, traditional methods of

characterization by washability analysis followed by dense media separation and (or) jigging technology may not be viable. The finer inter-growths of manganese minerals in gangue renders the ore more susceptible to a fines beneficiation approach.

New Developments

Coarse Processing and Waste Rejection

To reduce the rising production cost curve and improve sustainability of this strategic ore reserve, technology innovation throughout the value chain is imperative and needs to be constantly assessed.

Optimization of crushing methodology upstream should also be investigated because recent technology, for example high pressure grinding rolls (HPGR), has claimed to be more energy efficient as well as ideally suited for lower-grade, complex ores. The primary motivation for the use of HPGR as a hard rock comminution alternative is its energy efficiency when compared with conventional crushers and mills. Furthermore, downstream energy requirements, typically in ball milling, are often reduced due to the increased fineness of the HPGR product (compared with conventional crusher products) and to reduced work indices caused by micro-cracking of the HPGR product particles. Also known as micro-fracturing or micro-fissuring, this is the phenomenon whereby internal fracturing of particles occurs due to the extreme pressures exerted by the rolls in the compression zone. Being weakened, such particles display a reduced energy demand in the downstream comminution process as well as liberation benefits by cracking along grain boundaries.³⁰

Thermal pre-treatment of rocks before comminution has been shown to significantly reduce energy requirements for downstream milling and grinding processes.^{31,32} Recently the University of Adelaide in Australia has announced that they will be

researching the application of concentrating solar thermal heating for thermally assisted comminution.³³ Given the high quality of the solar resource, at an annual direct normal irradiance of 2800 kWh/m², at the location of the KMF leading to low solar thermal heating costs,³⁴ such a technology may find application at South African Manganese mines in the future.

Sorting technologies, being one of the oldest forms of beneficiation for upfront waste rejection, have grown substantially over the years. In the area of mineral beneficiation, the emergence of sensor-based sorting allows upgrading of low-grade ores to a level where more conventional processes become economically viable. X-ray transmission (XRT) and x-ray fluorescence (XRF) are seen as robust technologies that are used at mine sites in order to reject waste and upgrade feed material prior to transportation of material for further upgrade and beneficiation. When positioned correctly in a process flowsheet, considering that it is a dry processing technology, a pre-concentration stage or sensor-based ore sorting mechanism can reduce material transport costs, which essentially means that less waste is conveyed to the next part of the beneficiation process.

Most of the XRT solutions on the market recognize and separate materials based on their specific atomic density, allowing a high level of sorting purity irrespective of size, moisture or surface pollution, which renders the technology ideal for manganese sorting, provided feed material contains free waste. The application of sensor-based sorting is aimed at stimulating the sector by upgrading ores to a level where they can be viably exploited.³⁵

Fines Beneficiation

As high-grade material becomes depleted, we are slowly left with more complex and lower-grade material. With this comes the imminent need to re-evaluate and develop alternative fines beneficiation techniques or technologies.

Quantitative mineralogical assessment via electron microprobe analysis (EMPA) and mineral liberation analyzer (MLA) is conducted to determine the elemental composition of specific minerals, create a minerals database, and map individual particles in a fines sample. The mapped data is modeled as part of a particle tracking analysis (PTA) approach. The approach consists of a number of stages:

- Combining the particle data to represent a single sample
- Sorting the data into size, density, assay, and minerals classes, which then assists with possible processing solutions
- Tracking of liberated minerals or phases per size class for the actual separation

This information can then be used to predictively model the performance of various gravity operations

and their expected efficiencies and, regarding complex ores, predetermine possible process solutions. The model is Excel-based using proprietary spreadsheets and algorithms developed at Mintek.

A reflux classifier (RC) is a combination of a lamellar settler, autogenous dense medium separator and a fluidized bed separator (FBS) (Fig. 4a). It is ideally suited to fine and ultrafine beneficiation. The unit is able to tolerate changes in feed-grade variations, viscosity, and % solid more readily, offering an advantage in gravity separation and particle size classification. The footprint is much smaller than spirals and a full-scale unit can run up to 100 t/h. The unit can handle < 2 mm particles with a top:bottom size preferably at 4:1. Reflux classifiers were first applied in the coal industry but have since penetrated into the ferrous minerals industry.

DMS application is one of the most efficient processing options for lumpy manganese upgrade (> 1 mm). It is well documented that material finer than 1 mm reports significant deterioration in efficiency with the breakaway size for particles < 1 mm. Preliminary test work conducted on alternative media (water and gas atomized FeSi) has revealed potential to significantly upgrade low-grade or fine (-1 + 0.212 mm) material using ultra high density dense medium separation (UHDDMS) (Fig. 4b). Low DMS feed media relative densities in the order of 3.4–3.6 g/cm³ are thus required to achieve high density cut points of over 4.0 g/cm³ whilst maintaining stability within the plant. This modified application has entered the Fe ore industry specifically to reprocess tailings and low-grade material; there exists, therefore, potential to process manganese ore in a similar way.

SINTERING OF FINES

The brittle nature of manganese ores leads to a large amount of fines (< 6 mm) generated during sizing and transport of the ore.¹ Due to the burden nature of blast furnaces and submerged arc furnaces, fines are limited in the feed to ferromanganese alloy production furnaces and the need arises for an agglomeration technology. The current practice is to sinter manganese ore fines.

Historic Processing

There are currently two manganese ore sinter plants in South Africa. Both are situated next to manganese mines. The market for manganese sinter is both local and for export.

The older manganese sinter plant is at the Mamatwan mine.^{12,36} This sinter plant has been in operation since 1987 and is rated to produce 500,000 t/a. The sinter plant originally produced sinter from the Mamatwan mine carbonate-rich ores but was later used to sinter the upgraded product of dense medium separation. The newer plant is at the Kalagadi manganese mine and was

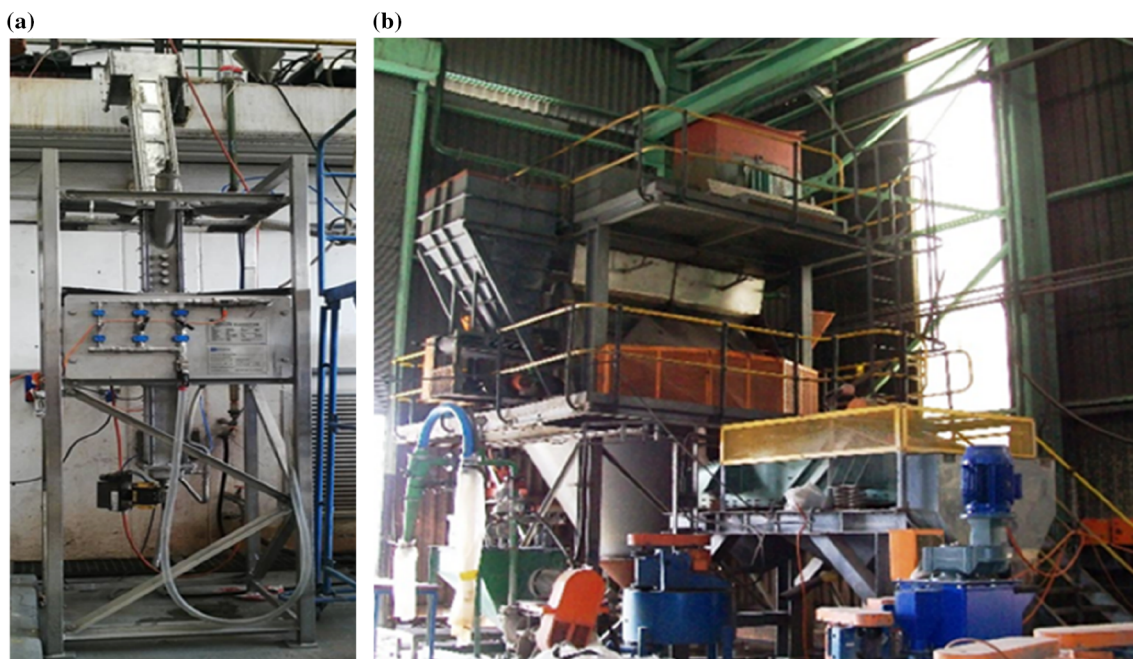


Fig. 4. (a) RC 100 classifier and (b) UHDDMS

built to produce 2.4 million tons of manganese ore sinter annually and opened in December 2012. This flowsheet does not include dense medium separation, but energy recovery is practised by preheating air for the ignition furnace burners through the sinter cooling strand.

Both the Mamatwan and the Kalagadi sinter plants are based on traveling grate sinter technology.

State of the Art

The state of the art manganese sinter plants use energy recovery from the sinter strand cooling to preheat air for the ignition furnace. Coke breeze is often preferred as the carbon source due to its lower cost compared with metallurgical coke. Manganese sinter operations have been well described^{12,37–39} in previous publications. The main unit operations in the sinter process are the sizing of the ore to < 6 mm, the mixing of the ore with water and solid reductant to form the green sinter mix, and the ignition of the green sinter mix in the ignition furnace followed by the sintering of the ignited mixture on the sinter strand while air is drawn through the sinter bed. Sintering occurs along a burn front and is completed before the hot sinter is discharged to the sinter cooling belt and re-sized for sale (sized to $+ 19$ mm and $- 75$ mm). A layer of previously sintered material covers the sinter belt and protects it from the hot sinter (Fig. 5).

New Developments

Energy efficiency in manganese sinter plants might be improved by similar plant modifications

as have been introduced in iron ore sintering.^{40,41} These improvements have been achieved by increasing the use of waste heat for feed preheating by selective waste gas recirculation, the use of coke oven gas to lower use of solid reductants when collocated with blast furnaces, and modifications to use lower-grade carbon reductants by using a separate combustion chamber for low-grade reductants and using the carbon-monoxide-rich off-gas for sinter production. Options also exist for sinter plants collocated with smelting facilities to feed hot sinter to smelters to reduce electricity requirements in smelting.

More recently, the integration of solar thermal energy to displace fossil fuels has been proposed. In particular, the use of solar thermal energy to preheat feed material or burner air to the ignition furnace,^{39,42} and thus reduce the consumption of diesel, promises a reduction in operational costs as well as greenhouse gas emissions. In the current low interest rate environment, capital intensive technologies such as concentrating solar benefit from lower financing costs may indeed offer an option to reduce carbon tax liability in the future and lower greenhouse gas emissions in an industry that was previously seen as hard to abate.

Research into carbonaceous ore sinter quality maintenance during and after transport, especially during long-distance marine transport or stockpiling in humid environments, may be warranted. Marine transport carries the risk that some oxides may hydrate, and form hydrated compounds. An example of such a reaction would be the hydration of calcium oxide to calcium hydroxide. The formation of hydrides weakens the physical strength of the

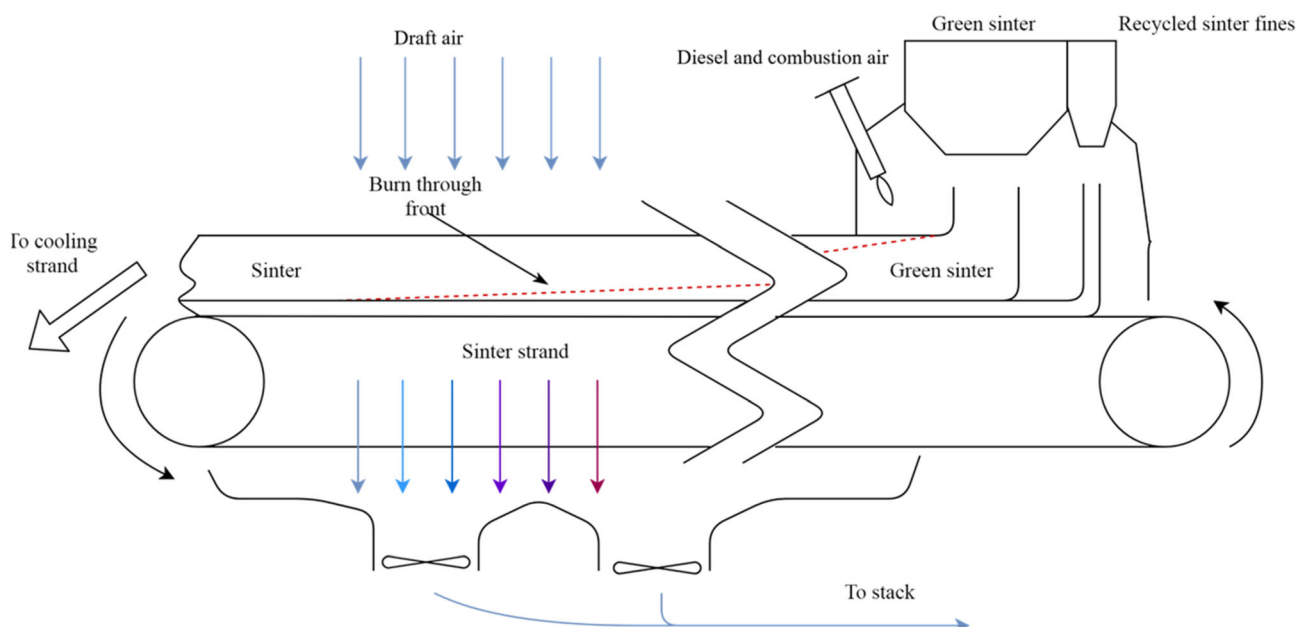


Fig. 5. The feed arrangement of a sinter strand including the ignition furnace and travelling grate

sinter, and volume changes due to hydride formation and can lead to cracking, reduction of compression strength and reduction of sinter size. In the iron ore industry these reasons have led to the avoidance of long distance transport of iron ore sinter, with preference given to indurated iron ore pellets when long transport is required.

Alternatives to the sinter process, such as pelletizing, have been proposed.⁴³ Pelletizing generally refers to the agglomeration of materials mixed with a binder and indurated or heated to strengthen the pellets. Although energy savings are obtained by the lower temperature requirements (1100 °C for manganese ore pellets compared with 1200–1300 °C for manganese ore sinter), increased comminution is required for pelletizing, negating these energy savings; therefore, sintering of manganese ore fines is still considered the state of the art agglomeration technology.

Given the imperative to reduce greenhouse gas emissions to net zero to curb global warming, research into a carbon neutral agglomeration method for manganese ore fines is required. Hydrogen combustion may be an alternative heating method for carbon-neutral pellets if the cost of green hydrogen production can be justified and safely demonstrated. Ensuring the energy efficiency of agglomeration methods, replacing fossil fuels as the energy source for agglomeration with solar or other renewable energy sources, and even replacing carbon with alternative reductants are all research directions aimed at reducing the environmental footprint of manganese ore fines agglomeration. The alternative would be changing the smelting step to a technology that can accept fine material. To the authors' current knowledge, no such alternative to

high-temperature smelting in blast furnaces or submerged arc furnaces exists: open bath technologies lead to high manganese losses to the dust due to fuming of manganese. Electrolytic manganese production is more expensive and currently reserved for a small but growing market for high purity manganese in battery applications.

ALLOY PRODUCTION

To produce the primary alloys, HCFeMn and SiMn, carbo-thermic reduction processes are applied. In these processes, manganese-bearing raw materials are reduced by solid carbon reductants to produce alloy, slag, and off-gas.^{1,43} MCFeMn is produced by blowing HCFeMn with (diluted) oxygen in a converter or by silico-thermic reduction of a synthetic slag, rich in MnO, in a shaking or mixing ladle process.

Historic Processing

Commercial production of ferromanganese containing 65% Mn started in France in 1875, using blast furnace (BF) technology.⁴⁴ In 1877 the Terre Noire Co in France produced ferromanganese containing 80% Mn and 6–7% carbon.⁴⁵ From 1890, ferromanganese could also be produced by electric submerged arc furnace (SAF),⁴⁴ but for the first half of the 20th century all ferromanganese was produced in BFs.¹ BFs use 4–6 times as much coke per ton of ferromanganese as do SAFs so, due to the high cost and scarcity of coke and the relative high capital investment required to build a BF, SAFs started to replace BFs in the second half of the 20th century. Today, most manganese ferroalloys are produced using SAFs.⁴⁵

In South Africa, the African Metals Corporation (Ammcor) Ltd started to produce HCFeMn in a BF with a hearth diameter of 10 ft in Newcastle in 1937. In 1942, HCFeMn was produced in a 3 MVA, rectangular arc furnace, with two refining furnaces for the production of MCFeMn. In 1951, operations relocated to Meyerton and today the plant is known as Metalloys. Assmang's Cato Ridge plant was commissioned in 1957 near the eponymous town. Transalloys, based in today's eMalahleni, was commissioned as a ferrochrome production plant in the 1960s but converted to SiMn in 1967.⁴⁶

State of the Art

Flowsheet Options

From a slag chemistry perspective, three distinct processes are in operation. HCFeMn is produced either by using a discard slag practice or in the duplex process. In the discard slag practice, the slag produced is discarded as waste. In the duplex process, the slag produced in the HCFeMn production is used as the main source of manganese in the subsequent SiMn production process. In terms of slag chemistry, the main difference lies in the basicity (B_4) and resulting MnO content of the slag (Table III). The slag basicity is again primarily dependent on the basicity of the ores used as the source of manganese. As the carbonate-rich, Mamatwan ore forms the basis of the smelter operations in South Africa, the discard slag practice is applied with quartz added as flux only to increase the fluidity of the slag.⁴⁷ SiMn in South Africa is produced from manganese ores as well.⁴⁸ Slag produced in SiMn production is discarded, irrespective of the processing route followed.

$$B_4 = \frac{\%CaO + \%MgO}{\%Al_2O_3 + \%SiO_2} \quad (1)$$

The SAF designs can be open, closed, or semi-closed. A closed furnace has a sealed roof with no or very little air ingress and the furnace off-gases are therefore not combusted. The roof of an open furnace is not sealed, and furnace off-gas is combusted on top of the furnace bed. A semi-open furnace is similar to an open furnace, but with doors installed between the furnace rim and roof to reduce air ingress and heat losses.

Off-gas collected from a closed furnace is rich in CO, and also contains CO₂ and H₂. Dust is removed from the gas by a wet scrubbing system. The dust, in

the form of a slurry, is pumped to settling dams. The cleaned gas is available as fuel for preheating of ladles or for combustion in a power generation plant. Off-gas collected from an open furnace is combusted on top of the burden and therefore poses no explosion risk. The gas is typically cooled by a water-cooled duct and trombone system and dust is removed by cyclone and bag-house systems. Dust collected can either be discarded as waste or recycled to the furnace via a briquetting plant.^{49,50}

The typical alloy compositions are summarized in Table I. SAFs are equipped with single- or bi-level tap-holes through which alloy and/or slag streams are tapped intermittently. With single-level tap-holes, alloy and slag are tapped as a single stream from the SAF. The stream runs via a launder into a ladle from which slag overflows into a slag pot (Fig. 6a). The ladle containing the alloy is transferred by overhead crane to a skimming area where any slag remaining is skimmed. The ladle is then transferred to a layer casting pit where the contents of 3–4 ladles are cast (Fig. 6b). Once cooled down, a front-end loader collects the alloy for screening at the alloy treatment plant. Alloy size fractions are specified in the respective standards (ASTM-A99 and ASTM-A483). Slag is allowed to cool in the slag pot and then tipped at the slag dump. Skimmed slag is collected with sculls from the launder and ladle and taken to a metal recovery plant. Recovered metal is either blended with the final saleable product or recycled to the SAF via a briquetting plant.^{49,50} For bi-level tapping systems, alloy is tapped into a ladle from a dedicated tap-hole and slag into a slag-pot from another dedicated tap-hole. Post tap-hole treatment can be similar to that of single-level tapping, but in some instances alloy is taken to a casting strand to be cast into pigs instead of being cast in layers.

Cost Drivers

The two main cost drivers for the production of manganese ferroalloys, apart from ore, are the prices of reductant and of electricity.^{1, 48,51}

Metallurgical-grade manganese ores contain more than 35% Mn and ferruginous ores 15–35% Mn, with high levels of Fe.⁴³ From Table II, one can see that the ores commercially exploited in South Africa are all considered metallurgical-grade ores. The smelters feed blends of ores, the choice driven by chemical properties, i.e., the Mn/Fe ratio typically estimated at 80% Mn recovery and 100% Fe

Table III. Typical chemical composition (mass%) and process temperature of slag tapped from the furnace during the production of manganese ferroalloys¹ with B_4 defined in Eq. 1

	SiO ₂	Al ₂ O ₃	MnO	MgO	CaO	B_4	Process temperature (°C)
HCFeMn—discard	24	21	15	5	35	0.9	1400–1450
HCFeMn—duplex	24	13	40	6	17	0.6	1400–1450
SiMn	45	16	9	9	21	0.5	1500–1600

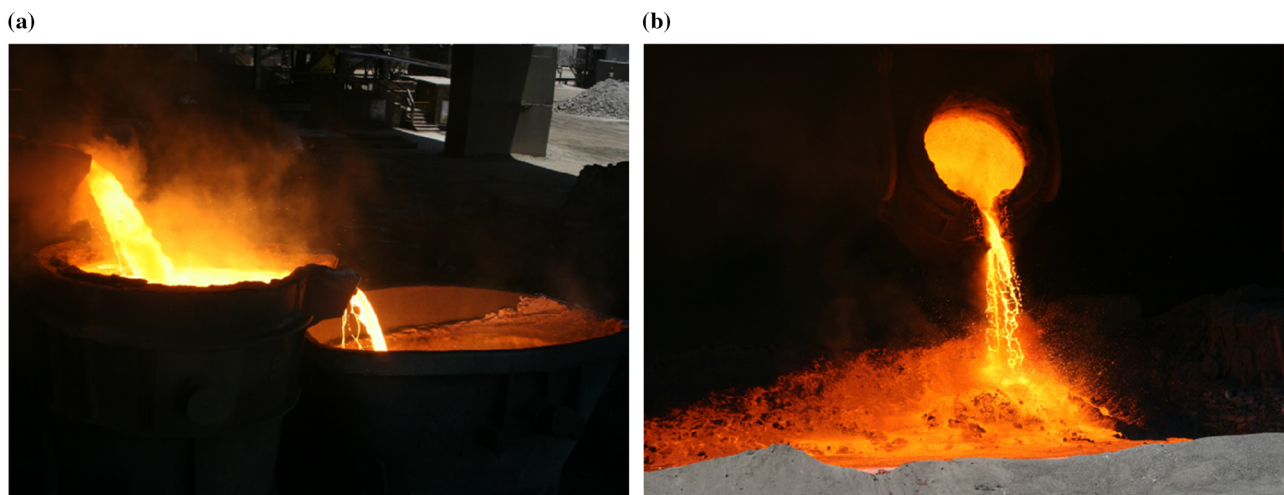


Fig. 6. (a) Slag and alloy being tapped from a single-level tap-hole running via a launder into a ladle with slag overflowing from the ladle into the slag pot and (b) alloy pouring from a ladle whilst being layer cast in a casting pit

recovery to the alloy; physical properties, i.e., particle size distribution; and price of ores.^{47,49,50} As smelters are situated around 600 km or more from the mines, ore does break down during rail transportation. The < 6 mm fraction is sieved from the bulk ore at the smelters, mixed with smelter dust collected from the off-gas cleaning plant, alloy fines generated in and collected from the crushing and screening plant, and binders, to form briquettes which are recycled to the smelters.⁴⁹

For carbonaceous reductants, smelters in South Africa feed a blend of bituminous coal which is sometimes supplemented with coke or anthracite.^{49,50} The handling of volatile matter condensing in the downstream gas cleaning facilities sometimes limits the amount of bituminous coal that can be included in the blend. Reductant properties of importance, other than the proximate analyses (determined as per ASTM-D3172: Standard Practice for Proximate Analysis of Coal and Coke) and ash composition, include reactivity with CO₂ and slag, electrical resistivity, and thermal strength.⁵²

For HCFeMn production, the typical electrical energy requirement ranges between 2200 kWh/ton and 3200 kWh/ton and for SiMn production, 3800 kWh/ton and 4300 kWh/ton.⁴³ The SAFs are typically circular with three Söderberg electrodes in an equilateral arrangement. Inside the furnace, electrical energy is dissipated from the electrodes to the process through a combination of resistive heating of a wet coke-bed (Fig. 7), consisting of slag and carbonaceous reductant, and arcing.⁵³ Typically, production furnaces carry loads of 15–45 MW.⁴³

Installed Capacity

Currently, South Africa has an installed capacity of about 900,000 tons per annum of ferromanganese alloys, applying SAF technology in the production of

HCFeMn and SiMn (Table IV). MCFeMn is produced at two sites using converter technology.

Installed capacity at Metalloys consists of four closed SAFs, two of which are rated at 75 MVA and two at 81 MVA, for the production of HCFeMn, and a 30-t top-blown bottom-stirred converter for MCFeMn production.⁴⁶ Installed capacity at Assmang's Cato Ridge plant consists of one 24-MVA semi-open, one 24-MVA closed, two 22-MVA semi-open, two 12-MVA closed SAFs, and a 30-t converter.⁴⁶ Installed capacity at Transalloys includes two 21-MVA open, one 23-MVA semi-open, and two 48-MVA semi-open SAFs.⁴⁹

New Developments

Manganese ferroalloy production is a significant producer of CO₂ emissions especially when the electrical energy utilized is produced in coal-fired power stations. For HCFeMn production, the generic CO₂ emission factor is estimated at 1.3 ton CO₂/ton alloy and for SiMn production at 1.4 ton CO₂/ton alloy.⁵⁴ In South Africa, electricity is mainly generated through coal-fired power stations and the CO₂ emissions associated are estimated at 862 g CO₂/kWh.⁴⁵ This adds an additional 1.9–2.8 tons CO₂/ton HCFeMn alloy and 3.3–3.7 tons CO₂/ton SiMn alloy. The EU-funded PreMa project (2018–2022), investigates the potential for a preheating stage to reduce the electrical energy requirement and CO₂ emissions produced during the production of HCFeMn in an SAF. The aim is to utilize industrial off-gases, bio-carbons, and/or solar thermal energy in order to reduce the consumption of fossil carbonaceous reductants as well as the overall energy consumption by 20%.

Overall process energy consumption can also typically be reduced with process scale-up. Conventional three-electrode, circular alternating current (AC)-based SAF manganese ferroalloy smelters are characterized by low resistance and

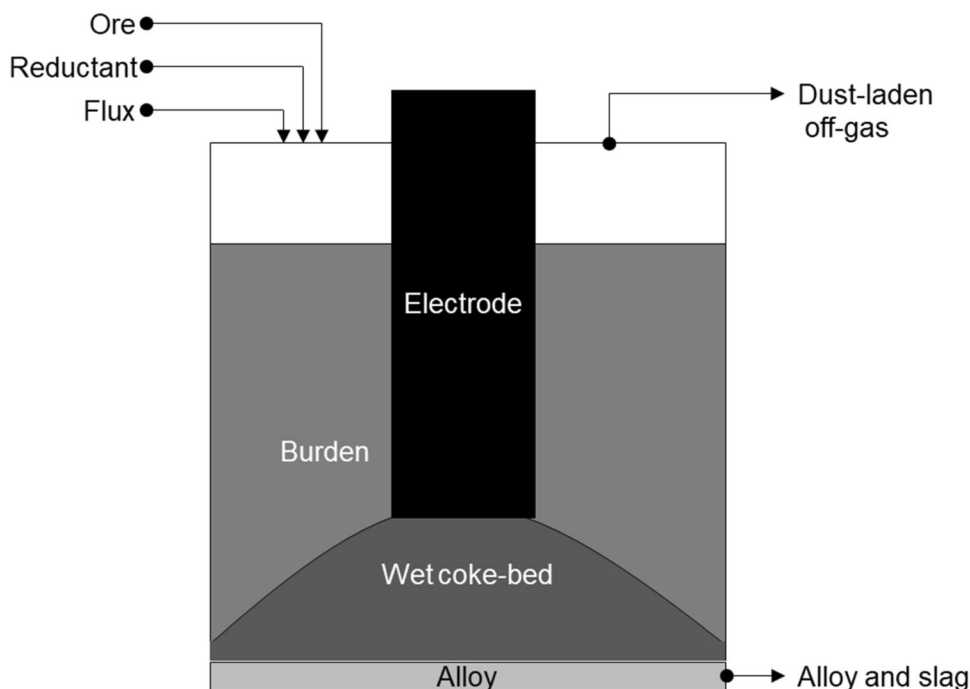


Fig. 7. Simple schematic of the process flow in an SAF utilized in the production of HCFeMn or SiMn (Adapted from Ref. 47)

Table IV. Installed capacity for manganese ferro-alloys in South Africa

Operating company	Commodity	Production rate (t/a)	MVA installed
Metalloys	HCFeMn	480,000	312
Assmang Cato Ridge	HCFeMn	240,000	116
Transalloys	SiMn	180,000	161
Total		900,000	589

thus high currents. Scale-up of such smelters would necessitate larger diameter electrodes to avoid exceeding the current carrying capacity and associated risk of electrode breakages. Increased electrode diameter, however, reduces furnace resistance and increases magnetic inductance or reactance, which has a compounding effect on reducing the power factor and energy efficiency. Additionally, for power factors between 0.65 and 0.80, a phenomenon known as the “interaction effect” becomes significant, resulting in the control of the operation becoming unmanageable. While the scale-up of a conventional AC SAF is limited, this should not be the case for a direct current (DC) smelter as electromagnetic inductance creates reactance only with alternating current. A further benefit of a multi-electrode large-scale DC SAF smelter would be the fact that there would be no reactance in the electric circuit(s), with associated benefits in terms of greater power generating capacity. Preliminary research and test work comparing AC and DC operations has been undertaken by Mintek, which show the DC configuration to be a viable, if not favorable alternative.⁵⁵

Another interesting development will be the evaluation of methane (and hydrogen) reduction of manganese ores and the effect on smelter operation at a pilot scale. Work at a laboratory scale demonstrated the possibility of reducing manganese ores to manganese carbides in the temperature range 1000–1200°C using methane gas or methane gas enriched in hydrogen.^{56,57} Manganese carbide formation is thermodynamically not possible in the CO-gas-rich atmospheres prevailing in the burden of the SAFs, and therefore much higher processing temperatures are required.

CONCLUSION

The manganese reserves currently being mined in the KMD produce metallurgical grade ores, which are readily reduced in existing SAF technology. In some instances minerals processing steps are applied, but in many instances these steps only consist of screening. Ore fines are not readily treatable in SAFs and sintering of ore fines is applied as the main agglomeration technique. Primary manganese ferroalloys, namely HCFeMn and SiMn, are produced in SAFs. Although these are

mature technologies, the processes are electrical energy intensive and produce significant amounts of CO₂ gas. In order to make the production of manganese ferroalloys more sustainable, projects are underway that are looking into upgrading of low-grade ores, agglomeration of ore fines in ways that are environmentally friendly, reduction of CO₂ emissions, and reduction of electrical energy consumption.

ACKNOWLEDGEMENTS

This paper is published with permission from Mintek.

REFERENCES

1. S.E. Olsen, M. Tangstad, and T. Lindstad, *Production of Manganese Ferroalloys* (Trondheim: Tapir Academic Press, 2007).
2. The Editors of Encyclopædia Britannica, *Manganese* (Encyclopædia Britannica, Inc., 2020), <https://www.britannica.com/science/manganese>. Accessed 6 Mar 2020.
3. L. Reijnders, *J. Clean. Prod.* (2016). <https://doi.org/10.1016/j.jclepro.2016.05.073>.
4. USGS, *Manganese Data Sheet—Mineral Commodity Summaries 2020* (United States Geological Survey, 2020), <http://pubs.usgs.gov/periodicals/mcs2020/mcs2020-manganese.pdf>. Accessed 6 Mar 2020.
5. R. Reisfeld, in *Encyclopedia of Materials—Science and Technology* (New York: Elsevier, 2001), p. 6472.
6. T. Kohga, M. Imamura, J. Takahashi, N. Tanaka, and T. Nishizawa, *JOM* (1995). <https://doi.org/10.1007/BF03221339>.
7. G. Savage, *Pottery* (Encyclopædia Britannica, Inc., 2019), <https://www.britannica.com/art/pottery>. Accessed 6 Mar 2020.
8. H. Bessemer and H. Bessemer, in *Sir Henry Bessemer, F.R.S.: An Autobiography* (London: Offices of Engineering, 1905), p. 256.
9. *The Annual Register, Or a View of the History, Politics, and Literature for the Year 1799* (London, 1799), p. 546.
10. *Repertory of Patent Inventions and Other Discoveries and Improvements in Arts, Manufactures and Agriculture* (London: J.S. Hodson, 1839), p. 317.
11. W.T. Lankford, N.L. Samways, R.F. Craven, and H.E. McGannon, in *Making, Shaping and Treating of Steel*, 10th edn. (Pittsburgh: Association of Iron and Steel Engineers, 1985), p. 407.
12. P.C. Pienaar and F.P. Smith, *A Case Study of the Production of High-Grade Manganese Sinter from Low-Grade Mamatwan Manganese Ore* (INFACON VI, 1992), <https://pyrometallurgy.co.za/InfaconVI/1131-Pienaar.pdf>. Accessed 20 Mar 2020.
13. J.D. Steenkamp, W.G. Bam, E. Ringdalen, M. Mushwana, S.A.C. Hockaday, and N.A. Sithole, *J. S. Afr. Inst. Min. Metall.* 118, 645 (2018).
14. J. Gutzmer and N.J. Beukes, *Econ. Geol.* 90, 823 (1995).
15. D. Chetty and J. Gutzmer, *Quantitative Mineralogy to Address Energy Consumption in Smelting of Ores from the Kalahari Manganese Field, South Africa* (INFACON XV, 2018), <https://www.pyrometallurgy.co.za/InfaconXV/Chetty.pdf>. Accessed 31 Mar 2020.
16. J. Gutzmer, *Genesis and Alteration of the Kalahari and Postmasburg Manganese Deposits, Griqualand West, South Africa* (University of Johannesburg, 1996), <http://hdl.handle.net/10210/5803>. Accessed 30 Mar 2020.
17. A.P. Du Plooy, *Randse Afrikaanse Universteit, Johannesburg, South Africa*, Unpublished Research, 2002.
18. A.S.E. Kleyenstüber, *Randse Afrikaanse Universteit, Johannesburg, South Africa*, Unpublished Research, 1985.
19. D. Chetty and J. Gutzmer, *Quantitative x-ray Diffraction as a Tool for Smelting Optimisation of Kalahari Manganese Ores* (AUSIMM, 2008), <https://ausimm.com/product/quantitative-x-ray-diffraction-as-a-tool-for-smelting-optimisation-of-kalahari-manganese-ores/>. Accessed 30 Mar 2020.
20. L.C. Blignaut, *A Petrographical and Geochemical Analysis of the Upper and Lower Manganese Ore Bodies from the Kalahari Manganese Deposit, Northern Cape, South Africa—Controls on Hydrothermal Metasomatism and Metal Upgrading* (University of Johannesburg, 2017), <http://hdl.handle.net/10210/233924>. Accessed 30 Mar 2020.
21. N.J. Beukes, in *Iron-Formation Facts and Problems*, vol. 6, eds. A. F. Trendall and R. C. Morris (New York: Elsevier, 1983), p. 131.
22. C.J. Nel, N.J. Beukes, and J.P.R. De Villiers, in *Mineral Deposits of Southern Africa*, ed. C.R. Anhaeusser, and S. Maske (Johannesburg: Geological Society of South Africa, 1986), p. 963.
23. D. Chetty, *A Geometallurgical Evaluation of the Ores of the Northern Kalahari Manganese Deposit, South Africa* (University of Johannesburg, 2008), <http://hdl.handle.net/10210/3223>. Accessed 30 Mar 2020.
24. M. Tangstad, K. Ichihara, and E. Ringdalen, *Pretreatment Unit in Ferromanganese Production* (INFACON IV, 2015), <https://www.pyrometallurgy.co.za/InfaconXIV/099-Tangstad.pdf>. Accessed 30 Mar 2020.
25. M. Tangstad, M. Sibony, S. Wasboe, and R. Tronstad, *Kinetics of the Prereduction of Manganese Ores* (INFACON IX, 2001), <https://www.pyrometallurgy.co.za/InfaconIX/202-Tangstad.pdf>. Accessed 30 Mar 2020.
26. D. Chetty and J. Gutzmer, in *Process Mineralogy. JKMRM Monograph Series in Mining and Mineral Processing* (Brisbane: Julius Kruttschnitt Mineral Research Centre, 2016), p. 402.
27. J.D. Steenkamp, G.M. Denton, and T. Pieters, *TMS Annual Meeting* (2020). https://doi.org/10.1007/978-3-030-36540-0_28.
28. R.C.A. Minnitt, *J. S. Afr. Inst. Min. Metall.* 114, 63 (2014).
29. V. Kivinen, H. Krogerus, and J. Daavittila, *Upgrading of Mn/Fe Ratio of Low-Grade Manganese Ore for Ferromanganese Production* (INFACON XII, 2010), <https://www.pyrometallurgy.co.za/InfaconXII/467-Kivinen.pdf>. Accessed 30 Mar 2020.
30. C. Morley, *J. S. Afr. Inst. Min. Metall.* 110, 107 (2010).
31. L.M. Tavares and R.P. King, *KONA Powder Part J.* (1999). <https://doi.org/10.14356/kona.1999023>.
32. A. Somani, T.K. Nandi, S.K. Pal, and A.K. Majumder, *Int. J. Min. Sci. Technol.* (2017). <https://doi.org/10.1016/j.ijmst.2017.01.013>.
33. G. Nathan, *Solar Thermal for Mineral Processing* (University of Adelaide, 2019), <http://www.adelaide.edu.au/research/news/list/2019/10/21/solar-thermal-for-mineral-processing>. Accessed 31 Mar 2020.
34. L. Hockaday, *Solar Thermal Applications in Minerals Processing in South Africa* (SASEC, 2019). <https://www.sasec.org.za/papers2019/76.pdf>. Accessed 31 Mar 2020.
35. C. Robben and H. Wotruba, *Minerals* (2019). <https://doi.org/10.3390/min9090523>.
36. W.A. Gericke, *The establishment of a 500 000 t/a Sinter Plant at Samancor's Mamatwan Mine* (INFACON V, 1989), <https://www.pyrometallurgy.co.za/InfaconV/024-Gericke.pdf>. Accessed 31 Mar 2020.
37. J. Malan, W. Barthel, and B.A. Dippenaar, *Optimizing Manganese Ore Sinter Plants: Process Parameters and Design Implications* (INFACON X, 2004), <https://pyrometallurgy.co.za/InfaconX/057.pdf>. Accessed 31 Mar 2020.
38. J. Daavittila, H. Krogerus, P. Oikarinen, and R. Sarkkinen, *Sintered Manganese Ore and Its Use in Ferromanganese Production* (INFACON IX, 2001), <https://www.pyrometallurgy.co.za/InfaconIX/212-Jorma.pdf>. Accessed 31 Mar 2020.
39. S.A.C. Hockaday, F. Dinter, and T.M. Harms, *Introducing Solar Thermal Heat into Minerals Processing: A Case Study on Replacing a Diesel Burner at a Sinter Plant* (SASEC, 2018), https://www.sasec.org.za/full_papers/74.pdf. Accessed 31 Mar 2020.

40. S. Hotzinger, M. Boberl, K. Czermal, T. Kornberger, and L. Gould, *New sinter plant at Dragon Steel, Taiwan* (Millennium Steel, 2011), http://millennium-steel.com/wp-content/uploads/2014/02/pp19-23_ms11.pdf. Accessed 31 Mar 2020.
41. S. Yamaguchi, T. Fujii, N. Yamamoto, and T. Nomura, *KOBELCO Pelletizing Process* (Kobelco Technology Review, 2010), https://www.kobelco.co.jp/english/ktr/pdf/ktr_29/058-068.pdf. Accessed 31 Mar 2020.
42. M. Lubkoll, S.A.C. Hockaday, and T.M. Harms, *Integrating Solar Process Heat into Manganese Ore Pre-heating* (SASEC, 2018), https://www.sasec.org.za/full_papers/57.pdf. Accessed 31 Mar 2020.
43. M. Tangstad, in *Handbook of Ferrous Alloys—Theory and Technology* (Oxford: Butterworth-Heinemann, 2013), p. 221.
44. J.H. Downing, *Manganese Processing* (Encyclopædia Britannica, Inc. 2013), <https://www.britannica.com/technology/manganese-processing>. Accessed 31 Mar 2020.
45. L. Holappa, in *Handbook of Ferrous Alloys—Theory and Technology* (Oxford: Butterworth-Heinemann, 2013), p. 9.
46. J. Basson, T.R. Curr, and W.A. Gericke, *South Africa's Ferro Alloys Industry—Present Status and Future Outlook* (INFACON XI, 2007), <https://www.pyrometallurgy.co.za/InfaconXI/003-Basson.pdf>. Accessed 31 Mar 2020.
47. J.D. Steenkamp, *TMS Annual Meeting* (2020), https://doi.org/10.1007/978-3-030-36540-0_67.
48. J.D. Steenkamp and J. Basson, *J. S. Afr. Inst. Min. Metall.* 113, 667 (2013).
49. J.D. Steenkamp, P. Maphutha, O. Makwarela, W.K. Banda, I. Thobadi, M. Sitefane, J. Gous, and J.J. Sutherland, *J. S. Afr. Inst. Min. Metall.* (2018). <https://doi.org/10.17159/2411-9717/2018/v118n3a13>.
50. N.A. Sithole, N. Rambuda, J.D. Steenkamp, D.A. Hayman, and C.J. Hockaday, *J. S. Afr. Inst. Min. Metall.* (2018). <https://doi.org/10.17159/2411-9717/2018/v118n11a11>.
51. H.J. Van Zyl, W.G. Bam, and J.D. Steenkamp, *J. S. Afr. Inst. Min. Metall.* (2020). <https://doi.org/10.17159/24119717/341/2020>.
52. M. Tangstad, J.P. Beukes, J.D. Steenkamp, and E. Ringdalen, in *New Trends in Coal Conversion—Combustion, Gasification, Emissions, and Coking*, ed. I. Suárez-Ruiz, M.A. Diez, and F. Rubiera (Oxford: Woodhead Publishing, Elsevier, 2019), p. 405.
53. J.D. Steenkamp, C.J. Hockaday, J.P. Gous, and T.W. Nzima, *JOM* (2017). <https://doi.org/10.1007/s11837-017-2434-3>.
54. T. Lindstad, S.E. Olsen, G. Tranell, T. Færden, and J. Lubetsky, *Greenhouse Gas Emissions from Ferrous Alloy Production* (INFACON XI, 2007), <https://www.pyrometallurgy.co.za/InfaconXI/457-Lindstad.pdf>. Accessed 31 Mar 2020.
55. H. Lagendijk, B. Xakalashé, T. Ligege, P. Ntikang, and K. Bisaka, *Comparing Manganese Ferrous Alloy Smelting in Pilot-Scale AC and DC Submerged-Arc Furnaces* (INFACON XII, 2010), <http://www.mintek.co.za/Pyromet/Files/2010Lagendijk.pdf>. Accessed 30 June 2020.
56. N. Anacleto, O. Ostrovski, and S. Ganguly, *ISIJ Int.* 44, 1480 (2004).
57. A. Bhalla and R.H. Eric, *Reduction Behavior of Manganese Ore Using Methane Gas* (INFACON XIV), <https://www.pyrometallurgy.co.za/InfaconXIV/461-Bhalla.pdf>. Accessed 30 June 2020.

Publisher's Note Springer Nature remains neutral with regard to jurisdictional claims in published maps and institutional affiliations.